

Conductivity profiles corresponding to the knee model and relevant SR spectra

H.J. Zhou¹, M. Hayakawa², Yu.P. Galuk³, A.P. Nickolaenko⁴

¹School of Information Engineering, Harbin Institute of Technology, Weihai, China.

²Hayakawa Institute of Seismo Electromagnetics Co. Ltd.,
The University of Electro-Communications Incubation Center, and
Advanced Wireless & Communications Research Center (AWCC)
The University of Electro-Communications, Tokyo, Japan

³Saint-Petersburg State University, Saint-Petersburg, Russia

⁴A.Ya. Usikov Institute for Radio-Physics and Electronics, NASU, Kharkov, Ukraine

E mail (hongjue_zhou@sina.com.cn, galyuck@paloma.spbu.ru, hayakawa@hi-seismo-em.jp, sasha@ire.kharkov.ua).

Accepted: 16 September 2015

Abstract: There are many models describing ELF radio propagation in the uniform Earth-ionosphere cavity. One of the most popular models is the knee model by Mushtak and Williams (2002). Unfortunately, this model only verbally describes the relevant conductivity profile of atmosphere, which is obligatory in the direct computational techniques. We introduce a conductivity profile based on this description and derive the related frequency dependence of complex propagation constant $\nu(f)$ using the rigorous full wave solution (FWS). Then, for the first time the Schumann resonance (SR) spectra for the same atmospheric conductivity profile are compared to those by different computational techniques. In two of them we use the formal zonal harmonic series representation (ZHSR) for the fields with the propagation constant $\nu(f)$ found either from the knee model formulas or from the FWS for the relevant conductivity profile. The third technique is based on the direct three-dimensional finite difference time domain (FDTD) technique with the same conductivity profile. Comparison reveals that the FWS and FDTD results are practically coincident in the whole SR band. The knee model spectra are close to those of FWS and FDTD data in the vicinity of the first SR mode, whereas deviations from the rigorous solutions proportionally increase with the frequency. Special attention is paid to the characteristic heights of ionosphere that provide coincident results for the FDTD spectra and the ZHSR spectra with FWS propagation constant.

© 2016 BBSCS RN SWS. All rights reserved

Key words: Schumann resonance, knee model, conductivity profile, full wave solution, finite difference time domain technique

1. Introduction

In the standard description of the sub-ionospheric radio wave propagation in extremely low frequencies (ELF: 3 Hz – 3 kHz), the propagation constant $\nu(f)$, the angular source–observer distance θ , and the current moment of the dipole source are necessary. Vertical electric and horizontal magnetic fields are found from the following expressions in the horizontally uniform isotropic Earth–ionosphere cavity under the $\exp(+i\omega t)$ time dependence (e.g. Galejs, 1972; Nickolaenko and Hayakawa, 2002, 2014):

$$E_r(\omega) = \frac{M_C(\omega) i \nu(\nu+1) P_\nu[\cos(\pi-\theta)]}{4ha^2 \varepsilon \omega \sin \pi \nu} = -\frac{M_C(\omega) i \nu(\nu+1)}{4\pi \varepsilon ha^2 \omega} \sum_{n=0}^{\infty} \frac{(2n+1) P_n(\cos \theta)}{n(n+1) - \nu(\nu+1)} \quad (1)$$

$$H_\theta(\omega) = -\frac{M_C(\omega) P_\nu^1[\cos(\pi-\theta)]}{4ha \sin \pi \nu} = \frac{M_C(\omega)}{4\pi ha} \sum_{n=1}^{\infty} \frac{(2n+1)}{n(n+1) - \nu(\nu+1)} P_n^1(\cos \theta) \quad (2)$$

where a is the Earth's radius; θ is the angular distance from the source; $M_C(\omega)$ is the current moment of the

vertical dipole source being independent of frequency; $\nu(f)$ is the propagation constant; h is the effective height of the ionosphere; $P_\nu[\cos(\pi-\theta)]$ and $P_\nu^1[\cos(\pi-\theta)]$ are the Legendre and associated Legendre functions of complex order ν . The vertical electric dipole source of the field is positioned at the pole ($r=a$, $\theta=0$) of the spherical polar coordinate system (r , θ , φ) with the origin at the Earth's center. The Legendre functions are expanded into infinite series on the Legendre polynomials regarded as zonal harmonic series representation (ZHSR). Such series were suggested and used for computations of the Schumann resonance (SR) fields with an account of 200 terms by Jones (1970). Later, the presentations were obtained with accelerated convergence, and the relevant material might be found in Nickolaenko and Hayakawa (2002, 2014). In the present paper, we use the Jones and Burke (1990) acceleration algorithm.

The role of propagation constant is especially important, which depends on the atmospheric conductivity profile up to about 100 km. Therefore, significant efforts were directed to its precise deducing. For this purpose, the models of stratified multi-layered ionosphere were used (Jones, 1967, Hynninen and Galuk, 1972, Bliokh et al., 1977,) that exploited the full wave solution (FWS). This approach was rather complicated since it demanded extended

computations, which was a serious obstacle in the pre-PC era. Besides, the knowledge of the conductivity of mesosphere was rather poor, therefore, the "engineering" formulas were used for the $\nu(f)$ functions based on the SR observations. The simplest, although precise enough one, was the linear dependence (see Nickolaenko and Hayakawa, 2002, 2014). The commonly accepted nonlinear frequency dependence $\nu(f)$ of the propagation constant has been suggested by Ishaq and Jones (1977) as shown in the following equations:

$$\nu(f) = [0.25 + (kaS)^2]^{1/2} - 0.5, \quad (3)$$

$$S = c/V - i \cdot 5.49 \cdot \eta/f, \quad (4)$$

$$c/V = 1.64 - 0.1759 \cdot \ln(f) + 0.01791 \cdot [\ln(f)]^2, \quad (5)$$

$$\eta = 0.063 \cdot f^{0.64}. \quad (6)$$

where f is the frequency in Hz, k is the free space wave number, S is the complex sine of the Brillouin waves propagating in the Earth-ionosphere waveguide (e.g., Wait, 1970), V is the phase velocity of radio wave, and η is the parameter accounting for the wave attenuation. For the $\exp(+i\omega t)$ time dependence, the positive sign of the root in equation (3) must be chosen, which guarantees attenuation of propagating radio waves. We use equations (3)–(6) in the following as the standard reference model.

It is obvious from the above that both in the field computations and in the interpretation the atmospheric conductivity profile $\sigma(h)$ is redundant. One can use the regular expressions (1)–(6) and compute the electromagnetic fields for the given current moment of the source and the ionosphere effective height h . But when solving the SR problem with the numeric techniques, like the finite difference time domain (FDTD) technique which has been widely used in the past decade for modeling the ELF wave propagation in the Earth-ionosphere cavity supported by the fast development of the computer resources (Hayakawa and Otsuyama, 2002; Otsuyama et al. 2003; Otsuyama and Hayakawa, 2004; Simpson and Taflove, 2004; Yang and Pasko, 2005, 2006, 2007; Navarro et al, 2008; Simpson et al., 2006; Zhou et al., 2013a, 2013b, Zhou and Qiao, 2015), one has to introduce the atmospheric conductivity profile $\sigma(h)$ within the altitudes from 0 to 100 km. Unfortunately, such information is scarce. Knowing this, the paper aims to suggest a conductivity profile of the regular atmosphere that might be applied in the FDTD computations.

In this paper, since the formal problem of finding the $\nu(f)$ dependence for an arbitrary conductivity profile $\sigma(h)$ remains unresolved, we will address the approximate nature of the $\nu(f)$ models first, including the single-scale exponential model, two-scale exponential model, and the knee model. Among these, the knee model is believed to be the most accurate one in the SR range, but there is no conductivity profile $\sigma(h)$ corresponding to the successful heuristic knee model. By using the verbal description of the knee model by Mushtak and Williams (2002), we will construct the corresponding profile of atmospheric

conductivity $\sigma(h)$ and apply this function in the FDTD technique. Concurrently with the formulas of the knee model by Mushtak and Williams (2002), the propagation constant $\nu(f)$ will be found using rigorous FWS. The SR spectra will be obtained and compared to those by corresponding three different techniques. In two of them we use the formal ZHSR for the fields with the propagation constant $\nu(f)$ found from the knee model formulas and from the FWS for the relevant conductivity profile. The third one is based on the rigorous direct FDTD technique with the same conductivity profile. For the first time the comparison is made of computational data obtained in direct FDTD technique and in the framework of classical FWS-ZHSR for the same atmospheric conductivity profile. The characteristic height of ionosphere in the ZHSR formulas will be discussed in the end.

2. Approximate models of conductivity profile and ELF propagation parameter

2.1. Single-scale exponential model

The approximate link between the propagation constant $\nu(f)$ at a fixed extremely low frequency f (ELF: 3-3000 Hz) with parameters of the exponential profile $\sigma(h)$ for the flat geometry was suggested by Greifinger and Greifinger (1978). Long before this work, the exponential conductivity profile of the lower ionosphere was used at very low frequencies (VLF: 3-30 kHz) (Wait and Spies, 1964, Galejs, 1972). However, transition to ELF has completely changed the way in which the parameters of the profile were used. The approximate relations for the $\nu(f)$ function were suggested by Greifinger and Greifinger (1978) after detailed rigorous analysis of the problem. These formulas involved the so-called "electric" and "magnetic" characteristic heights of the particular $\sigma(h)$ profile and relevant scale heights at these altitudes.

The lower, "electric" height h_E at a given frequency f is found from the condition that the conduction and displacement currents are equal at this height. This means that the point is found at a given conductivity profile where the following condition is held:

$$\sigma_E(h_E) = \omega \epsilon_0, \quad (7)$$

where $\omega = 2\pi f$ is the circular frequency and $\epsilon_0 = 8.854187 \times 10^{-12}$ F/m is the permittivity of free space.

The upper, "magnetic" height h_M is found in a similar way. At this altitude the wavelength in the plasma at the frequency f is equal to the local scale height ζ_M , so that the condition acquires the following form:

$$\sigma_M(h_M) = [4\mu_0 \omega \zeta_M^2]^{-1}, \quad (8)$$

where $\mu_0 = 4\pi \times 10^{-7}$ H/m is the permeability of free space. After finding the characteristic heights and height scales, one can calculate the complex propagation constant:

$$\text{Re}[\nu] = ka \sqrt{h_M/h_E} \quad (9)$$

$$\text{Im}[\nu] = ka (\zeta_E/h_E + \zeta_M/h_M) \pi/4. \quad (10)$$

Thus, the procedure of deriving the propagation constant at a particular frequency includes manual

finding of the two heights and two scale heights at a given profile and substituting these into equations (9) and (10).

Such a procedure is universal: it might be used for an arbitrary profile. However, it is time consuming and inconvenient in use. This is why Greifinger and Greifinger (1978) suggested the following relation for finding the magnetic characteristic height:

$$h_M = h_E - 2\zeta_E \ln(2k\zeta_E). \quad (11)$$

This relation has a clear physical meaning. The electric field of a radio wave penetrates to the height h_E . Further diffusion of the magnetic field into the plasma depends on the local "electric" scale height ζ_E .

When one treats a profile having the constant scale height, equation (11) provides the upper characteristic height coincident with that found from equation (8). When the scale height varies with altitude, the magnetic height found from (11) becomes a convenient proxy of the real height satisfying condition (8).

Greifinger and Greifinger (1978) derived the characteristic heights h_E and h_M and the scale heights ζ_E and ζ_M for the Cole and Pierce (1965) profile, and this allowed obtaining the realistic propagation constants matching the measurements of ELF radio signals transmitted by the Wisconsin Test Facility (WTF), the US navy transmitter.

The exponential Greifinger and Greifinger (1978) model appeared to be rather convenient and efficient. A desire emerged to adopt it to the SR studies, and two obstacles should be overcome. The first one was the Cartesian geometry used in the original exponential model while the SR takes place only in a closed spherical volume. This obstacle was overcome by proving that relations remain valid in the spherical Earth-ionosphere cavity, provided that the signal frequency exceeds a few hertz (Nickolaenko and Rabinowicz, 1982, 1987).

The second problem was associated with the wide band nature of natural radio signals in distinction from the man-made ELF transmissions. SR signals cover approximately a decade of 4–40 Hz. A prospect of returning to the $\sigma(h)$ plot for every frequency was the second obstacle. This problem was solved by modifying the equations for the characteristic heights by introducing the reference height h_R and the reference frequency f_R . These quantities appeared in the papers evaluating feasible SR in the global cavities of other planets (Nickolaenko and Rabinowicz, 1982, 1987). The lower characteristic height as a function of frequency was introduced as:

$$h_E(f) = h_R + \zeta_E \ln(f/f_R), \quad (12)$$

and the upper characteristic height was found using equation (11). The following parameters were used for the Earth-ionosphere cavity: $f_R = 1$ Hz, $\zeta_E = 3.4$ km, and $h_R = 38.8$ km in Nickolaenko and Rabinowicz (1982). The atmosphere of the Venus corresponded to the following set: $f_R = 1$ Hz, $\zeta_E = 2.7$ km, and $h_R = 65.9$ km. The Earth-ionosphere cavity played the role of a reference model for validating the approach itself and

evaluating the accuracy of the modeling. Later, a similar approach was suggested by Sentman (1990, 1995) and Fullekrug (2000). Expediency of the ELF propagation constant found from a single-scale exponential profile model is based both on its simplicity and a possibility of putting forward the physically meaningful interpretation with rather realistic ionosphere models.

2.2. Two-scale exponential model

Further development of the single-scale exponential model was the introduction of the two-scale exponential profile. In the simplest variant, the characteristic heights were calculated from equations (12) and (11), but in the vicinity of magnetic height the scale height ζ_E was substituted by the ζ_M value. Such a profile was regarded as a two-scale profile. More sophisticated variants of two-scale profiles were also used (e.g. Sentman, 1995) having a bent $\sigma(h)$ dependence between 50 and 60 km altitude, which is often regarded as a "knee". Here, the transition occurs from the ionic conductivity at low altitudes to prevalence of electrons at higher altitudes (Kirillov, 1996, Kirillov et al., 1997, Kirillov and Kopeykin, 2002, Mushtak and Williams, 2002, Pechony and Price, 2004, Pechony 2007, Greifinger et al., 2007). These works described the procedure of obtaining the $\nu(f)$ dependence and the goal was the effective parameters of RLC transmission lines used in the two dimensional telegraph equations (2DTE) technique. Among these, the knee model introduced by Mushtak and Williams (2002) was suggested having the key distinction that two scale heights are used around the complex electric height while the complex magnetic height is introduced in a separate way, see the next sub-section.

2.3. Knee model

This knee model defines the following complex electric and magnetic heights h_E and h_M :

$$h_E(f) = h_{kn} + \zeta_a \ln(f/f_{kn}) + \ln[1+(f_{kn}/f)^2](\zeta_a - \zeta_b)/2 + i[\zeta_a \pi/2 - (\zeta_a - \zeta_b) \tan^{-1}(f_{kn}/f)] \quad (13)$$

and

$$h_M(f) = h_m^* - \zeta_m \ln(f/f_m^*) - i\zeta_m(f) \pi/2. \quad (14)$$

Here h_{kn} and f_{kn} are the knee height and knee reference frequency correspondingly. Similarly to equation (7), these parameters introduce the coordinates of the "knee" (the altitude and the relevant conductivity). The detailed description of a knee profile might be found in Greifinger et al. (2007). Two scale heights are valid around the knee: ζ_a is the scale height above the knee and ζ_b is the scale height below the knee, usually $\zeta_a < \zeta_b$ (see Table 1).

Equation (14) separately defines the upper characteristic height. It implies the magnetic reference height h_m^* and the magnetic reference frequency f_m^* . The frequency dependent magnetic scale height is introduced by the following equation:

Table 1. The empirical values of the parameters in the knee model (Mushtak and Williams, 2002)

f_{kn} , Hz	h_{kn} , km	ζ_b , km	ζ_a , km	f_m^* , Hz	h_m^* , km	ζ_m^* , km	b_m , km Hz
10	55	8.3	2.9	8	96.5	4.0	20

$$\zeta_M = \zeta_m^* + b_m(1/f - 1/f_m^*), \quad (15)$$

where ζ_m^* is the reference scale height, and b_m is the coefficient controlling frequency variations of the upper scale height.

The propagation constant $\nu(f)$ is obtained from the regular expression for the heuristic ELF models (Greifinger and Greifinger, 1978):

$$\nu(\nu+1) = (ka)^2 h_M / h_E, \quad (16)$$

or from the equation for the $\exp(+i\omega t)$ time dependence:

$$\nu(f) = [1/4 + (ka)^2 h_M / h_E]^{1/2} - 1/2 \quad (17)$$

Parameters involved in formulas (13)–(17) are listed in Table 1. They were specified by Mushtak and Williams (2002) to match alteration of the observed Q-factors with the mode number n of the SR.

2.4. Accuracy of exponential models

We emphasize that the above mentioned models are not based on the actual $\sigma(h)$ profile. Instead, they operate with a set of parameters that allow computing the propagation constant as a function of frequency, and these parameters are regarded as characteristic heights and scale heights.

Let the air conductivity $\sigma(h)$ be the exponential function of height over the ground $\sigma(h) = \sigma \exp(-h/\zeta)$. One may use the above listed equations for computing the ELF propagation constant $\nu(f)$. Simultaneously, one can construct the rigorous solution of the problem using the FWS (see below) and also derive the propagation constant. Owing to the approximate nature of equations (11) and (12), the "exponential" solution will deviate from the rigorous one. Knott (1998), and Jones and Knott (1999, 2003) addressed these deviations: they evaluated the propagation constant, the SR frequencies and the quality factors. It was shown that the exponential model deviates from the rigorous solution. The real part of propagation constant (or the phase velocity of radio waves) deviates only by 0.15 – 1.2 %, while the imaginary part (the wave attenuation factor) might depart by more than 10 %.

Similar deviations might be expected for the knee model. A set of profile parameters based on the knee model was introduced and applied by Pechony (2007) using the 2DTE technique. However, it was not emphasized that the RLC parameters of the 2D transmission line were obtained from the heuristic equations rather than the rigorous FWS. The solution thus obtained remains an approximate one, and the characteristic heights and scale heights may not correspond to an actual conductivity profile $\sigma(h)$ (Galuk et al., 2015). So, the model conductivity profiles based on the knee and heuristic exponential models provide unrealistic SR data when used in FDTD technique. We will make relevant computations in this

work to compare data of the knee model with the results of rigorous solutions.

3. The conductivity profile based on knee model

The conductivity profile of atmosphere is necessary when obtaining rigorous solutions using the FWS or the FDTD techniques, and this profile must exactly correspond to the heuristic knee model. Unfortunately, the works incorporating the knee model are only based on the verbal description of the $\sigma(h)$ profile. None of these depicts the conductivity profile nearby the both characteristic heights and demonstrates correspondence of the propagation constant found from the profile and from heuristic relations. Obtaining such a profile is not a simple task, especially because all model parameters are functions of frequency and some of them are complex functions.

We construct the $\sigma(h)$ function by using the knee model (Mushtak and Williams, 2002). The profile in the horizontally uniform Earth–ionosphere cavity combines two exponential functions around the "knee" altitude:

$$\sigma(h) = \begin{cases} \sigma_{kn} \exp\left[\frac{h-h_{kn}}{\zeta_b}\right] & \text{when } h < h_{kn} \\ \sigma_{kn} \exp\left[\frac{h-h_{kn}}{\zeta_a}\right] & \text{when } h \geq h_{kn} \end{cases} \quad (18)$$

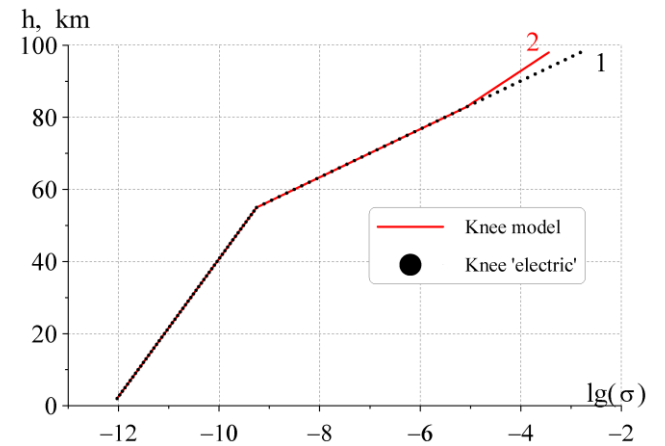


Fig. 1. Conductivity profiles corresponding to the knee model.

The reference frequency $f_{kn} = 10$ Hz and the knee altitude $h_{kn} = 55$ km were used by Mushtak and Williams (2002). We calculate the relevant knee conductivity $\sigma_{kn} = 2\pi\epsilon_0 f_{kn} = 5.5663 \cdot 10^{-10}$ S/m. The $\sigma(h)$ profile (18) is continued from the knee point (σ_{kn}, h_{kn}) by two exponents having the scale height ζ_b below the knee altitude and ζ_a above it. This function is shown in Fig.1 by black dots, and we regard it as "knee electric" or profile 1. Plots in Fig. 1 are shown in the standard way. The abscissa depicts the logarithm of conductivity, and the ordinate shows the altitude above the ground ranging from 0 to 100 km.

The higher part of the conductivity profile in the knee model must intersect with the magnetic altitude $h_M = 96.5$ km through the magnetic characteristic conductivity $\sigma_M(h_M) = 2.4737 \cdot 10^{-10}$ S/m according to equation (8). The profile linked to this upper point has the scale height of 4 km, and it intersects with the lower, "electric" part (profile 1) at about 83 km altitude. Thus, we obtain the $\sigma(h)$ dependence corresponding to the knee model in the whole 0–100 km interval. It is shown by the red line in Fig. 1, and we regard it as profile 2. For the $\lg(\sigma)$ shown on the abscissa, profile 1 is formed by two straight lines, and profile 2 is a composition of three intersecting straight lines. The profile 2 corresponding to the knee model contains the knee at 55 km altitude and an "anti-knee" at 83 km.

We suggest that profile 2 describes the same propagation condition in the uniform Earth-ionosphere cavity for all the models: the heuristic, the FWS, and the FDTD. Therefore, we apply it in the FWS computations of propagation constant, which will be compared with the standard Ishaq and Jones (1977) model and with the data obtained using the heuristic equations (13)-(17).

4. Full wave solution (FWS)

In a rigorous treatment of ELF radio propagation in a horizontally stratified medium, one obtains a system of linear algebraic equations for the wave transition and reflection coefficients in the adjacent layers (Wait, 1970, Galejs, 1972, Bliokh et al., 1977, 1980). The problem formulation in terms of the surface impedance is more convenient than the direct application of boundary conditions for the horizontal electric and magnetic fields at each boundary. By introducing the surface impedance at the interfaces, one obtains the first order differential equation (19). The solution of (19) is constructed numerically by iterations. Detailed description of particular procedures and the results obtained for a realistic conductivity profiles can be found in Hynninen and Galuk (1972), Bliokh et al. (1977), and Galuk and Ivanov (1978).

One obtains the following first order nonlinear equation for the spherical surface impedance when treating the eigen-value problem in the Earth-ionosphere cavity formed by the stratified plasma:

$$\frac{d}{dr} \delta(r) - ik\varepsilon(r)\delta^2(r) + ik + \frac{\lambda}{ikr^2\varepsilon(r)} = 0 \quad (19)$$

Here, $\delta(r)$ is the spherical surface impedance at the interfaces of the adjacent layers of atmosphere; $\lambda = v(v + 1)$ is the complex eigen-value; v is the propagation constant; k is the wave number $k = \omega/c$; c is the light velocity in vacuum; r is the radius-vector of the spherical polar coordinate system (r, θ, φ) , and it is defined on the semi-infinite interval $0 \leq r < \infty$; $\varepsilon(r) = 1 - i\sigma(r)/\omega\varepsilon_0$ is the complex relative dielectric constant of air; the $\exp(+i\omega t)$ time dependence is assumed.

The boundary conditions for the surface impedance must be formulated in addition to equation (19). The Earth is perfectly conducting at ELF,

and the first boundary condition is: $\delta(a) = 0$, where a is the Earth's radius. The ionosphere can be regarded as a uniform highly conducting medium starting from $r_1 = a + 100$ km, and the second boundary condition takes the form: $\delta(r_1) = [\varepsilon(r_1)]^{-1/2}$, where $|\varepsilon(r_1)| \gg 1$.

The eigen-value problem is finding the parameter λ from the nonlinear equation $\delta(a, \lambda) = 0$. The solution is obtained by numerical integration of equation (19) from r_1 to $r = a$. The function $\delta(a, \lambda)$ is analytic with respect to parameter λ , hence its roots can be found by iterations or by the Newton's method. Let λ^l be the l -th order iteration to the sought eigen-value λ , then the $(l + 1)$ -th iteration is:

$$\lambda^{l+1} = \lambda^l - \frac{\delta(a; \lambda^l)}{\frac{\partial}{\partial \lambda} \delta(a; \lambda^l)} \quad (20)$$

After obtaining the λ^l iteration, the integration of Eq. (19) along the height is repeated with the new eigen-value thus providing the next λ^{l+1} iteration. The process continues until the old and new eigen-values deviate by less than 10^{-7} .

The derivative $\delta_1(r) \equiv \frac{\partial}{\partial \lambda} \delta(r, \lambda)$ involved in formula (20) is obtained by integrating the supplementary differential equation. It was obtained by differentiating equation (19) by λ . This equation and the initial condition at $r = r_1$ are:

$$\frac{d}{dr} \delta_1(r) - 2ik\varepsilon(r)\delta(r)\delta_1(r) + \frac{1}{ikr^2\varepsilon(r)} = 0 \quad (21)$$

and

$$\delta_1(r_1) = 0 \quad (22)$$

The upper height in the ionosphere r_1 was chosen by exhaustive search: solutions were constructed for several r_1 values, and the value of 100 km was chosen since the final result stopped changing within the 10^{-7} accuracy with the increase above this height.

When calculating the field components, one has to derive both the eigen-values and the so-called integral norm N^0 . These quantities do not require additional computations in our scheme, since:

$$N^0 = ika^2 \frac{\partial}{\partial \lambda} \delta(a; \lambda) = ika^2 \delta_1(a) \cdot \quad (23)$$

The integral norm (23) provides the lower characteristic height of the cavity.

$$N^0 = h_c(f) = \frac{\int_a^\infty E_r(r) dr}{E_r(a)} = \int_0^\infty \frac{dh}{1 - i\sigma(h)/\omega\varepsilon_0} \cdot \quad (24)$$

To stress its distinction from the heuristic h_E found from (13), we use the notation h_c since this is the height allowing obtaining the elementary capacitance in the 2D RLC transmission line (Kirillov, 1996, Kirillov et al., 1997, Kirillov and Kopeykin, 2002). The upper (inductance) height h_L is defined as:

$$h_L = \frac{\int_a^\infty r H_\varphi(r) dr}{H_\varphi(a)} \cdot \quad (25)$$

To compute this height, we use the relation $\nu(\nu+1)=(k/a)^2 h_L/h_C$. The inductance h_L and the capacitance h_C heights have much in common with the Greifinger's characteristic heights, and these are completely similar to the magnetic and electric heights of the knee model. However, the Greifinger's heights are real, while h_L and h_C are complex. In distinction from the characteristic heights of the knee model, the h_L and h_C heights are found from the rigorous FWS for a conductivity profile. The frequency dependence $h_M(f)$ and $h_E(f)$ was simply postulated in the knee model by equations (13) and (14).

The propagation parameter, and the complex characteristic heights were obtained using the FWS procedure for the conductivity profile 2. The range of altitudes was 0–100 km and the step $dh = 1$ km was used in the computations. Fig. 2 depicts the frequency variations of complex heights in the knee model and derived by FWS.

Two frames are shown in Fig. 2. The upper one depicts frequency variations of the real part of characteristic height, and the lower one shows the imaginary part of these heights. Curves with squares and dots correspond to h_M and h_E relevant to the knee model (Mushtak and Williams, 2002), respectively. The line with triangles and the smooth line correspond to the FWS-derived h_L and h_C , respectively. Plots in Fig. 2 indicate that the knee model closely represents the results of the rigorous FWS for the electric characteristic height. Deviations are more pronounced in the magnetic height, although these are not great except deviations of $\text{Im}[h_M]$ from $\text{Im}[h_L]$. We observe that equations (13)–(14) closely correspond to the FWS for the knee profile.

Figure 3 compares the propagation constants of all above-mentioned models. Upper plot in Fig. 3 presents the imaginary part of propagation constant (the wave attenuation rate). Here, we depict the etalon dependence derived by Ishaq and Jones (1977) by the black smooth line and compare it with the knee model (red curve with dots) and FWS data (blue line with stars). The wave attenuations are practically coincident in the frequency band of the first three SR modes, but the standard model predicts somewhat lower attenuation rate above the 20 Hz frequency.

Lower plots in Fig. 3 present the real part of propagation constant (relevant to the wave propagation velocity) in the vicinity of the first, second, and third SR modes. One may observe that departures in the $\text{Re}[\nu(f)]$ plots become visible gradually at the higher modes. The peak frequency f_n of the n -th SR mode satisfies the condition $\text{Re}[\nu(f_n)] = n$ (Nickolaenko and Hayakawa, 2002, 2014). Therefore, intersections of particular plots with the levels $\text{Re}[\nu(f_n)] = 1, 2,$ and 3 in the lower frames of Fig. 3 indicate the position of corresponding peak frequencies. All models give close values of the real part of the propagation constant,

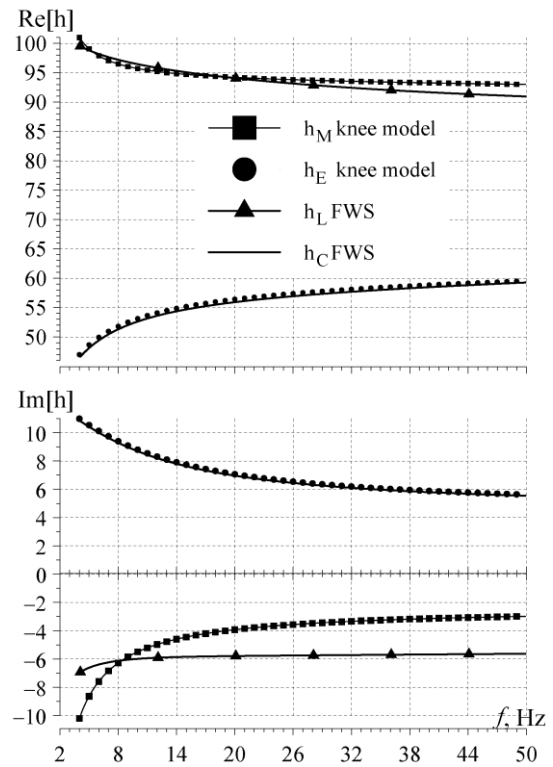


Fig. 2. Upper and lower characteristic heights against the frequency.

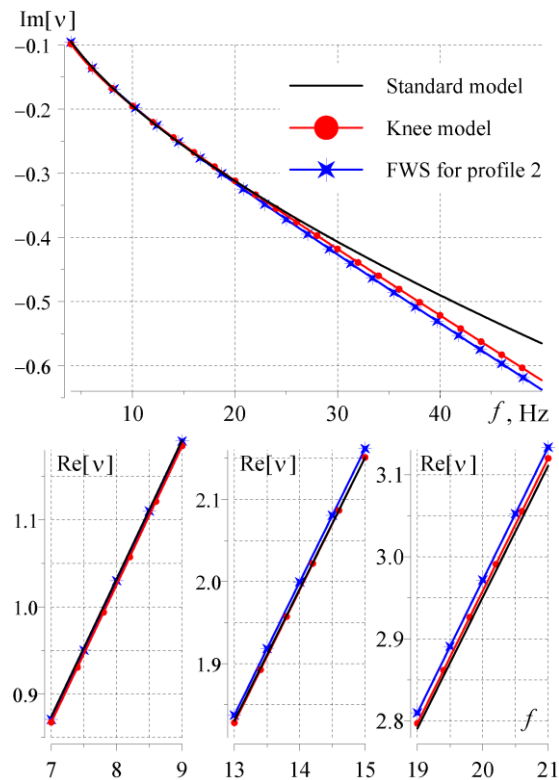


Fig. 3. Dispersion curves in the standard model (smooth black curve), knee model (red curve with dots), and FWS for the knee profile (blue curve with stars). Upper frame shows frequency variations of the imaginary part of the propagation constant (wave attenuation) and three lower frames depict frequency the $\text{Re}[\nu(f)]$ dependence in the vicinity of the first three SR modes.

Table 2. The theoretical modal frequencies and quality factors for the lower five SR modes with different models of propagation parameters

Mode number	Reference model (Ishaq and Jones,1977)		Empirical knee model (Mushtak and Williams,2002)		Conductivity profile 2	
	f_n (Hz)	Q_n	f_n	Q_n	f_n	Q_n
1	7.71	4.09	7.74	4.01	7.67	4.06
2	13.98	4.86	13.97	5.20	13.85	4.87
3	20.24	5.43	20.11	6.02	20.00	5.38
4	26.52	5.91	26.24	6.61	26.19	5.73
5	32.81	6.32	32.39	7.07	32.42	5.98

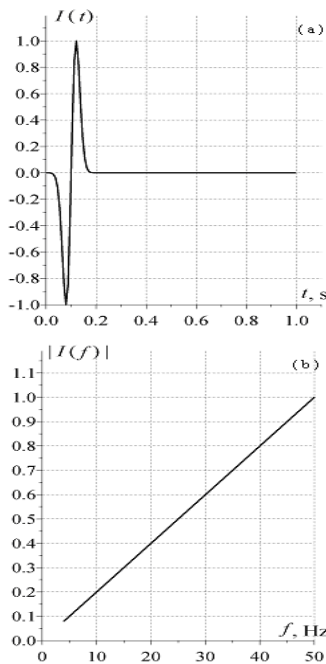


Fig. 4. The time waveform (a) and the spectra (b) of the vertical dipole used in the FDTD algorithm.

therefore, the peak frequencies are almost coincident for all three models, although departures become visible at higher modes. Deviations in the imaginary part or in the attenuation rate of radio waves also become obvious at higher modes.

We further calculate the theoretical modal frequencies f_n and quality factors Q_n for the lower five SR modes with the FWS-derived propagation parameter, and compare them with those calculated with the empirical knee model by Mushtak and Williams (2002) and the reference model by Ishaq and Jones (1977), as shown in Table 2. The following theoretical expressions for f_n and Q_n are used (Mushtak and Williams,2002):

$$f_n = f_n^{(0)} \frac{\text{Re} S(f_n)}{|S(f_n)|^2} \quad (26)$$

$$Q_n = \frac{\text{Re} S(f_n)}{2|\text{Im} S(f_n)|} \quad (27)$$

where $f_n^{(0)} = (c/2\pi a)\sqrt{n(n+1)}$ is the resonance frequency in the ideal Earth-ionosphere cavity.

From Table 2, the resonance frequencies of the three models are coincident, and the Q factors of our conductivity profile 2 are closer to those of the reference model compared with the empirical knee model by Mushtak and Williams (2002). Plots in Fig. 3 indicate that profile 2 provides the propagation constant very close to the reference model within the entire SR band: deviations in the phase velocity do not exceed 1%, and those in the attenuation rate are within the $\pm 5\%$ interval. Thus, profile 2 with the two bent regions (the knee and the anti-knee) is appropriate for modeling the global electromagnetic resonance in the Earth-ionosphere cavity. We speak here about its possible applications in the direct methods of field computations, such as FDTD, 2DTE and the transmission line matrix technique (Christopoulos, 1995; Morente et al.,2003,2004; Toledo-Redondo et al.,2013).

5. The FDTD method

The three-dimension (3D) spherical-coordinate FDTD technique with latitude-longitude grids is adopted here to obtain the direct solution for the conductivity profile 2. Its iterative equations are mainly derived from the differential form of the Maxwell equations, except the singularities at the poles, which are resolved using the integral form of the Maxwell's equations (Holland, 1983). The Earth-ionosphere cavity is assumed to be confined by two concentric spherical surfaces: the inner Earth's surface with the radius of 6370 km and the outer lower ionosphere surface at an altitude of 100 km. Both the boundaries are perfect conductors. The grid sizes are $\Delta r = 5$ km, $\Delta \theta = \Delta \phi = 1^\circ$ in r , θ , and ϕ directions, respectively. The time step is set as $\Delta t = \Delta r/(2c)$, where c is the light velocity in the vacuum. The conductivity profile 2 with the 2.5 km ($\Delta r/2$) step is used because E_r component is defined at the center of each grid in the vertical direction while E_θ and E_ϕ are defined at the extreme point of each grid. A vertical dipole is assumed to be the field source having the length of the cavity height positioned at the North pole.

The source current in the FDTD algorithm was selected to have the zero DC component, and it is shown in Fig. 4 together with its amplitude spectrum. In the ZHSR expressions (1) and (2), the current moment of the source was $M_c(f) = \text{const}$. To make the ZHSR and FDTD data compatible, the spectra obtained after Fourier transform of the FDTD time domain signal were divided by the source spectrum shown in Fig.4 (b).

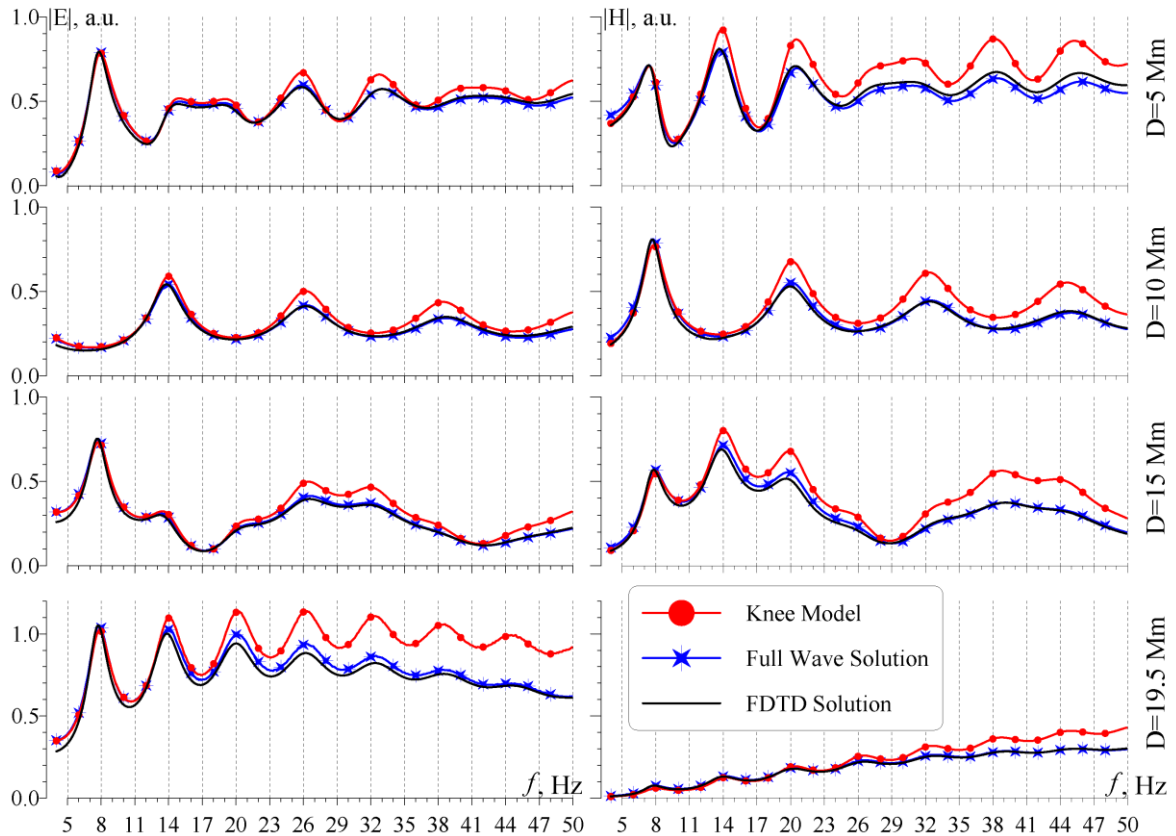


Fig. 5. Amplitude spectra of the vertical electric field and horizontal magnetic field at the discrete source-observer distances.

6. Comparison of the SR spectra

The major goal of our modeling was obtaining the ELF fields. We must remind here that deviations in propagation conditions become more obvious when one turns to the SR spectra rather than to the propagation constant (Nickolaenko and Hayakawa, 2002). Two schemes are used in this work: the ZHSR and FDTD technique. The spectra relating to the heuristic knee model by Mushtak and Williams (2002) are calculated with the ZHSR, and the spectra relating to the rigorous solutions (FWS and FDTD) for the conductivity profile 2 are calculated with both the methods.

Figure 5 depicts the computed amplitude spectra of the vertical electric field E_r and the horizontal magnetic field H_ϕ at a few source-observer distances of 5, 10, 15, and 19.5 Mm. The frequency from 4 to 50 Hz is plotted on the abscissa. The ordinates show the field amplitudes in arbitrary units being the same at all frames. The red lines with dots represent spectra calculated with the ZHSR algorithm using the knee model formulas (13)–(17). The blue lines with stars represent the ZHSR spectra calculated for the propagation parameters derived by FWS for the conductivity profile 2. The black smooth lines show spectra obtained by the FDTD procedure for the profile 2. Thus, the propagation model in the FWS-ZHSR and FDTD solutions is exactly the same.

For the first time the comparison is made of computational data obtained in direct FDTD

technique and in the framework of classical FWS-ZHSR for the same atmospheric conductivity profile. One may observe that in spite of applying completely different computation techniques, the amplitude spectra are practically coincident for the FWS-ZHSR and FDTD solutions. Mutual deviations are negligible. It is worth noting here that we used the ionosphere height $h = \text{Re}[h_E]$ in the both equations (1) and (2), and we will discuss this detail below. The knee model by Mushtak and Williams (2002) provides the results slightly deviating from the FWS-ZHSR and FDTD data. These departures proportionally increase with the frequency. Similarly to Nickolaenko and Hayakawa (2002), we observe that spectral patterns are more sensitive to deviations between the models than the relevant dispersion curves.

All spectra in Fig. 5 are similar. To note deviations, one has to plot all of them together. Visible departures of the solution based on the heuristic knee model from the rigorous FWS-ZHSR and FDTD spectra arise from the approximate nature of the knee model and its approximate interpretation of the equivalent conductivity profile. Similar deviations were reported by Knott (1998) and Jones and Knott (1999, 2003) relevant to the exponential Greifinger and Greifinger (1978) model.

In many applications these discrepancies are insignificant. However, there is an important area where accuracy of the field amplitude is crucial. We speak of deducing the spatial distribution of global thunderstorms from the simultaneous SR records

performed at the globally separated observatories. The method of tomographic reconstruction is used to accomplish this task (Shvets et al., 2010; Shvets and Hayakawa, 2011). The procedure is exceptionally sensitive to amplitudes of the basic functions (the spectral patterns for the different source distances). In particular, when one applies the basic functions corresponding to the heuristic knee model, the reconstruction will substantially underestimate the remote thunderstorm activity. Therefore, the recovered distribution of lightning strokes will become distorted. This is why the rigorous FWS-ZHSR and FDTD solutions should be preferred in the tomographic reconstructions.

7. Discussion

Visual departure of profile 2 from profile 1 in Fig. 1 allows us to predict the character of deviations of the relevant propagation constants. As we observe, profiles depart at altitudes above 83 km, and the air conductivity should be increased when one transfers from profile 1 to profile 2. The FDTD numerical experiments with the disturbed profiles (Yang and Pasko, 2005, Yang et al., 2006, Zhou and Qiao, 2015) indicate that such a “high altitude” modification increases the observed peak frequency of SR. Therefore, we argue that the FDTD models applying the profiles of type 1, which are widely used in the literature, will overestimate the resonance frequencies.

We have checked the consistency of the SR spectra obtained for the same conductivity profile when using the heuristic knee model, the FWS, and the FDTD technique. We found a close correspondence of the amplitude spectra derived by the rigorous FDTD and FWS-ZHSR techniques for the first time. The heuristic knee model also provides data close to the rigorous methods when one is interested in the ELF propagation constant within the SR band. Deviations in the amplitude spectra are much more pronounced.

The other important finding is the value of the effective ionosphere height exploited in the ZHSR. The ionosphere height is a real constant in the ideal cavity, and it was also assumed to be a constant in many studies of the cavity with the vertically non-uniform ionosphere. Sometimes, the effective height is associated with the lower and/or the upper characteristic heights when computing spectra of electric or magnetic fields. We found that the coincident SR spectra in the FDTD and FWS-ZHSR techniques are obtained when the ionosphere height is $h = \text{Re}[h_E]$ regardless the field component. (This statement is also valid when $h = |h_E|$ since the imaginary part of characteristic height is much smaller than its real part). We compare below the FWS-ZHSR results with those of FDTD for different ionosphere heights found for conductivity profile 2. The source-observer distance is 10 Mm. This is the nodal distance for the odd resonance modes in the electric field and for the even modes of magnetic field. Fig. 6 compares the vertical electric field spectra for $h = 60$ km, $\text{Re}[h_M]$, and $\text{Re}[h_E]$ heights used in the ZHSR formula (1). Fig. 7

depicts the horizontal magnetic field with $h = 60$ km, $\text{Re}[h_M]$, and $\text{Re}[h_E]$ heights in the ZHSR formula (2). Obviously, the effective cavity height $h = \text{Re}[h_E]$ fits the FDTD data in the best way regardless the particular field component. Deviations between the FDTD and ZHSR results for $\text{Re}[h_E]$ might arise from the different height steps used in the FWS ($dh = 1$ km) and the FDTD ($dh = 5$ km) numerical solutions. This point deserves a separate treatment.

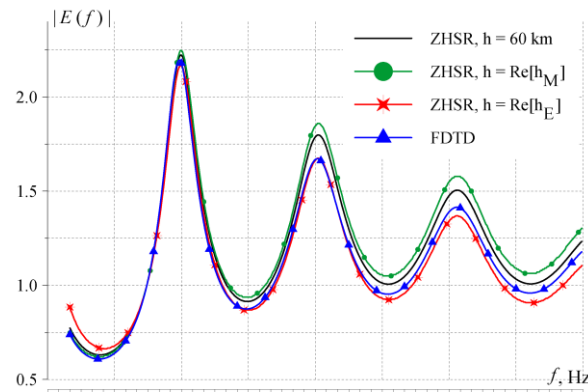


Fig. 6. Comparison of the vertical electric field spectra obtained with ZHSR and FDTD (blue line with triangles) under the same propagation condition. Three cases are shown: $h=60$ km (black smooth line), $\text{Re}[h_M]$ (green line with dots), and $\text{Re}[h_E]$ (red line with stars) relevant to the ZHSR formula.

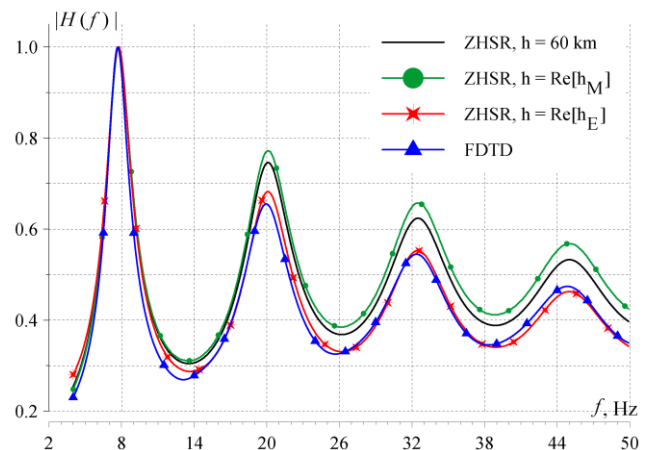


Fig. 7. Comparison of the horizontal magnetic field spectra obtained with ZHSR and FDTD (blue line with triangles) under the same propagation condition. Three cases are shown: $h=60$ km (black smooth line), $\text{Re}[h_M]$ (green line with dots), and $\text{Re}[h_E]$ (red line with stars) relevant to the ZHSR formula.

8. Conclusion

We constructed the conductivity profile based on verbal description of the knee model by Mushtak and Williams (2002), and computed the corresponding propagation constant by using the rigorous FWS. Comparison of propagation constant obtained by the FWS, from the Mushtak and Williams (2002) knee model, and from the standard Ishaq and Jones (1977) reference model showed their close correspondence.

The profile was used in two rigorous solutions of the problem: the FWS-ZHSR and the FDTD. For the first time

the comparison is made of computational data obtained in direct FDTD technique and in the framework of classical FWS-ZHSR for the same atmospheric conductivity profile. Exceptional similarity is demonstrated of the relevant amplitude spectra of the vertical electric and horizontal magnetic field components obtained by these two completely different approaches.

The SR spectra were also computed based on the heuristic knee model by Mushtak and Williams (2002) by using the ZHSR expressions. Comparison of spectra showed deviations of this solution from the rigorous results. Spectral departures gradually increase with frequency. This suggests that the heuristic knee model does not exactly correspond to its verbal interpretation.

It is found in addition that the ionosphere effective height involved in the ZHSR formula should be equal to the real part of electric characteristic height or to its modulus in spite of what a particular field component is computed, vertical electric or horizontal magnetic. This peculiarity indicates a necessity of special investigation in the future.

Acknowledgements

The research was funded by the Chinese National Natural Science Fund (61401116) and "the Fundamental Research Funds for the Central Universities" (grant HIT.NSRIF.2016101). The authors appreciate the helpful suggestions of the unknown reviewer.

References

- Bliokh, P.V., Nickolaenko, A.P., and Filipov Yu. F.: 1980, SRs in the Earth-ionosphere Cavity, Peter Peregrinus, Oxford-New York-Paris, p. 168.
- Bliokh, P.V., Galuk, Yu.P., Hynninen, E.M., Nickolaenko, A.P., and Rabinowicz, L.M.: 1977, *Izv. VUZOV, Radiofizika*. 20(4), 501.
- Christopoulos, C.: 1995, *The Transmission-line Modeling Method*, IEEE Press, Piscataway, p. 215.
- Cole, R.K., and Pierce, E.T.: 1965, *J. Geophys. Res.* 70(11), 2735.
- Fullekrug, M.: 2000, *Physics Letters A* 275(1), 80.
- Galejs, J.: 1972, *Terrestrial Propagation of Long Electromagnetic Waves*, Pergamon Press, Oxford-New York-Toronto-Sydney-Braunschweig, p. 362.
- Galuk, Yu.P., and Ivanov, V.I.: 1978, *Problems of Diffraction and Radio Wave Propagation* (in Russian), iss. 16, Leningrad State University, Leningrad, p. 148.
- Galuk, Yu.P., Nickolaenko, and A.P., Hayakawa, M.: 2015, *Radio-Physics and Electronics* 6(20), 41. (in Russian)
- Greifinger, C. and Greifinger, P.: 1978, *Radio Sci.* 13, 831.
- Greifinger P. S., Mushtak, V.C., and Williams, E.R.: 2007, *Radio Sci.* 42, RS2S12. doi:10.1029/2006RS003500, 2007.
- Hayakawa, M. and Otsuyama, T.: 2002, *ACES J.* 17(3), 239.
- Holland, R.: 1983, *IEEE Trans. Nucl. Sci.* NS-30 (6), 4592.
- Hynninen, E.M., and Galuk, Yu.P.: 1972, *Problems of Diffraction and Radio Wave Propagation* (in Russian), iss. 11, Leningrad State University, Leningrad, p. 109.
- Ishaq, M., and Jones, D. L.: 1977, *Electron Lett.* 13, 254.
- Jones, D.L.: 1967, *J. Atmos. Terr. Phys.* 29, 1037.
- Jones, D. L.: 1970, *Radio Sci.* 5, 803.
- Jones, D. L. and Burke, C. P.: 1990, *J. Phys. A. Math. Gen.* 23, 3159.
- Jones, D.L., and Knott, M.: 1999, *Comparison of simplified and full-wave ELF propagation models*, Abstracts of reports at URSI General Assembly, Toronto, Session E6.
- Jones, D.L., and Knott, M.: 2003, *Radiophysics and Electronics* 8(1), 55.
- Kirillov, V.V.: 1996, *Izv. VUZOV, Radiofizika* 39(12), 1103. (in Russian)
- Kirillov, V.V., Kopeykin, V.N., and Mushtak, V.C.: 1997, *Geomagnetism and Aeronomy* 37(3), 114. (in Russian)
- Kirillov, V.V., and Kopeykin, V.N.: 2002, *Izv. VUZOV, Radiofizika* 45(12), 1011. (in Russian)
- Knott, M.: 1998, *Computations of ELF EM fields in the Earth-ionosphere duct*. Report, Physics Dept., King's College, London, p. 45.
- Morente., J. A., Molina-Cuberos, G. J, Port, J. A, Besser, B. P, Salinas, A., Schwingenschuch, K., and Lichtenegger, H.: 2003, *J. Geophys. Res.* 108(A5), 1195. doi:10.1029/2002JA009779.
- Morente., J. A., Porti, J. A, Salinas, A., Molina-Cuberos, G. J, Lichtenegger, H., Besser, B. P, and Schwingenschuch, K.: 2004, *J. Geophys. Res.* 109, A05306. doi:10.1029/2002JA009779.
- Mushtak, V. C. and Williams, E. R.: 2002, *J. Atmos. Sol. Terr. Phys.* 64(18), 1989.
- Navarro, E. A., Soriano A., Morente, J. A. and Porti, J. A.: 2008, *J. Geophys. Res.* 113, A09301. doi: 10.1029/2008JA 013143.
- Nickolaenko, A.P., and Rabinowicz, L.M.: 1982, *Cosmic Research* 20(1), 67.
- Nickolaenko, A.P., and Rabinowicz, L.M.: 1987, *Cosmic Research* 25(2), 301.
- Nickolaenko, A.P., and Hayakawa, M.: 2002, *Resonances in the Earth-ionosphere cavity*, Kluwer Academic Publishers, Dordrecht-Boston-London, p. 380.
- Nickolaenko, A.P., and Hayakawa, M.: 2014, *SR for Tyros (Essentials of global electromagnetic resonance in the Earth-ionosphere cavity)*, Springer, Tokyo-Heidelberg-New York-Dordrecht-London, p. 348.
- Otsuyama, T., Sakuma, D., and Hayakawa, M.: 2003, *Radio Sci.* 38(6), 1103. doi: 10.1029/2002RS002752.
- Otsuyama, T. and Hayakawa, M.: 2004, *IEEJ. Trans. Fundamentals and Materials* 124(12), 1203. doi: 10.1541/ieejfms.124.1203.
- Pechony, O., and Price, C.: 2004, *Radio Sci.* 39, RS5007. doi:10.1029/2004RS003056.
- Pechony, O.: 2007, *Modeling and simulations of SR parameters observed at the Mitzpe Ramon field station*, Ph.D. Thesis, Tel-Aviv University, Israel, p. 92.
- Shvets, A. V., Hobara, Y., and Hayakawa, M.: 2010, *J. Geophys. Res.* 115, A12316.
- Shvets, A.V., and Hayakawa, M.: 2011, *Surv. Geophys.* 32(6), 705.
- Sentman, D.D.: 1990, *J. Atmos. Terr. Phys.* 52(1), 35.
- Sentman D.D.: 1995, in H. Volland (ed.), *SRs, Handbook of Atmospheric Electrodynamics*, CRC Press Inc., Boca Raton-London-Tokyo, p. 298.
- Simpson, J.J., and Taflove, A.: 2004, *IEEE Trans. Antenna Propag.* 52, 443. doi: 10.1109/tap.2004.823953.
- Simpson, J.J., Heikes, R.P., and Taflove, A.: 2006, *IEEE Trans. Antenna Propag.* 54(6), 1734. doi: 10.1109/tap.2006.875504.
- Toledo-Redondo, S., Salinas, A., Morente-Molinera, J.A., Mendez, A., Fornieles, J., Porti, J., and Morente, J.A.: 2013, *Journal of Computational Physics*, 236, 367.
- Wait, J.R., and Spies, K.P.: 1964, *NBS Technical Note* 300, 33.
- Wait, J.R.: 1970, *Electromagnetic Waves in Stratified Media*, Pergamon Press, Oxford. -New York-Toronto, p. 608.
- Yang, H., and Pasko, V. P.: 2005, *Geophys. Res. Lett.* 32, L03114. doi: 10.1029/2004GL021343.
- Yang, H., and Pasko, V. P.: 2006, *Radio Sci.* 41, RS2S14. doi: 10.1029/2005RS003402.
- Yang, H., and Pasko, V. P.: 2007, *Geophys. Res. Lett.* 34, L11102. doi: 10.1029/2007GL030092.
- Yang, H., Pasko, V.P., and Yair, Y.: 2006, *Radio Sci.* 41, RS2S03. doi: 10.1029/2005RS003431.
- Zhou, H., Yu, H., Cao, B., and Qiao, X.: 2013. a, *J. Atmos. Sol. Terr. Phys.* 98, 86. doi: 10.1016/j.jastp.2013.03.021.
- Zhou, H., Zhou Z., Qiao, X., and Yu, H.: 2013. b, *J. Geophys. Res. Atmos.* 118 (23), 13,338. doi: 10.1002/2013jd020269.
- Zhou, H. and Qiao, X.: 2015, *J. Geophys. Res. Atmos.* 120. doi: 10.1002/2014JD022696.